

Automatic Segmentation of Menisci in MR
Images Using Pattern Recognition and Graph
Cuts

Fredrik Nedmark, fredrik_n84@hotmail.com

April 14, 2011

Abstract

In this Master's thesis a system for automatic segmentation of the menisci in magnetic resonance (MR) images is developed and tested. MR imaging is a non invasive method with no ionization and with good soft tissue contrast and constitutes an important tool to evaluate soft tissue, tendon, ligaments and menisci in the knee. The menisci are located between the femur (thigh bone) and patella (shin bone) in the knee and has several functions, such as shock absorption. Medical imaging systems have been improved during the last decades. Images today are produced with higher resolution and faster acquisition time than before. Processing these images manually is very time consuming. Therefore it is necessary to create computerized tools that can be used by the medical staff in their work with diagnosis of illness and treatments of patients. The approach for constructing the automatically segment system is divided into three subparts. The first task is to extract all bone parts from the images. Secondly, the area where the menisci can be found is localized and the final step is to segment the menisci. This thesis is mainly based on two methods and they are pattern recognition with Laws' texture features and Graph Cut. In this thesis the system is tested on five examinations produced in Landskrona hospital from a Philips 1.5T machine using a spin-echo sequence. The result is promising and could with further work become an accurate system for automatically segmenting the menisci.

Acknowledgements

I would like to thank Magnus Tägil at the Department of Orthopedics in Lund for valuable comments, support and test materials. I would also like to thank my supervisors Kalle Åström and Petter Strandmark at the Mathematical Imaging Group at the Centre for Mathematical Sciences in Lund for their guidance, helpful comments and support.

Contents

1	Magnetic Resonance Images of the Knee	2
1.1	What is the Meniscus?	3
1.2	Magnetic Resonance Imaging (MRI)	3
1.3	Image Acquisition	6
1.4	Related Work	7
2	Theory	9
2.1	Laws' Texture Algorithm	9
2.2	Graph Cut	11
3	Segmentation Workflow	15
3.1	Segmentation of Bone	15
3.1.1	Create Classdata with Laws' Texture Algorithm	18
3.1.2	Segmentation Process for Segmenting Bone With Graph Cut	18
3.2	Find the Correct Localization of the Menisci	22
3.3	Segmentation of the Menisci	22
3.3.1	Finding the Mean Intensities of the Meniscus	23
3.3.2	Segmentation Process	25
4	Results	32
4.1	Result of Bone Segmentation	32
4.2	Result from Locating the Menisci Locations	33
4.3	Segmentation Result of the Menisci	34
4.4	Evaluation of the Results from the Automatic Segmentation	38
4.4.1	Examination 1	39
4.4.2	Examination 2	39
4.4.3	Examination 4	39
4.4.4	Examination 5	39
4.4.5	Examination 5 again	40
4.4.6	Summary	40
5	Future work	45

Chapter 1

Magnetic Resonance Images of the Knee

During the last several decades medical imaging systems have improved considerably. The systems have improved both in terms of better resolution and faster acquisition speed. Images have become a necessary part of today's patient care since they are used in diagnosis and treatment of patients. This is the reason why the number of produced images increases and why it is important to create computerized tools for their analysis. Computerized tools extract information that hopefully will help the medical staff with faster and more accurate analysis, cf. [7, page 1].

The aim of this Master's thesis is to automatically segment the menisci from a Magnetic Resonance Imaging (MRI) examination. MRI is a non-invasive method with no ionization and with good soft tissue contrast, cf. [7, page 18]. This Master's thesis was made in collaboration with Magnus Tägil at the Department of Orthopedics in Lund and the Mathematical Imaging Group at the Centre for Mathematical Sciences in Lund. The MR images that were used during this work were produced at the hospital in Landskrona. The approach during this thesis is mainly divided into three subparts. The first task is to extract all bone parts from the images. Secondly, the area where the menisci can be found is localized and the final step is to segment the menisci. Two main methods are used in this thesis: pattern recognition with Laws' texture features and Graph Cut.

The content of this thesis can be summarized as follows: Chapter 1 contains essential background information that is needed to understand the work that has been done. Chapter 2 covers the theory of different methods used in the work. Chapter 3 contains a description of the workflow of the program. Chapter 4 includes a discussion of the results. In chapter 5 future work is discussed.

1.1 What is the Meniscus?

The basic anatomy of the human knee bone parts is shown in figure 1.1. In these images the major bone parts are visible from different angles. The left image shows the frontal view also known as the coronal plane, see figure 1.2 for more information about the discussed body planes. The right image shows the sagittal view of the knee. Bone parts of interest are the femur, tibia and patella. The meniscus shape is well known and looks like a crescent shaped object of fibrocartilage that is located between the surfaces of the femur and tibia, see figure 1.3. In a normal human knee two menisci can be found, one lateral and one medial. The name reflect the location where the menisci can be found. The lateral meniscus is located on the outside of the knee and the medial on the inside. This is visible in figure 1.3 and 1.4. Figure 1.4 shows the meniscus from the transverse plane. From this figure both menisci are visible from above. In figure 1.3 the knee is shown in the frontal plane and the location of the meniscus is pointed out with an arrow. Also observe the meniscus horns that has been pointed out in figure 1.3 but is still fully visible in figure 1.4. The meniscus horns plays a major part in this thesis. In the sagittal view the horns have a characteristic triangular shape, which can be used when trying to locate the meniscus.

The meniscus plays an important role for biomechanical functions. As previously stated, it is located between the femur and tibia, therefore one essential purpose is to act as load bearer and shock absorber. This is also the reason for why the loss of meniscus increases the risk of developing osteoarthritis in the knee since the forces are distributed on a smaller area. Other important tasks are helping stabilizing the knee joint and lubrication of the joint surfaces, cf. [15, 6].

1.2 Magnetic Resonance Imaging (MRI)

MRI is a non invasive technique with no ionizing radiation that creates high quality images of the inside of the human body. To create images of the structures inside the body the nuclear spin of the hydrogen atoms are used. By adding a strong external static magnetic field, about 1-10 T, the majority of the hydrogen atoms have their spin pointing in the same direction creating the magnetization vector which precess around the static magnetic field at the resonance frequency. An external electromagnetic radio frequency (RF) pulse at the resonant frequency is transmitted. The RF pulse will flip the magnetization vector into the plane perpendicular to the static magnetic field where the signal can be detected.

Echo time, T_e , is the time between the RF pulse and the time when the signal is detected. For more detailed information regarding how the MR works see [7]. There are mainly two important properties. First of all the proton density and secondly the two relaxation times called spin-lattice and spin-spin relaxation time are of interest. These relaxation times are also called T1 and T2 respectively. The relaxation time is a measure of how long time it takes for

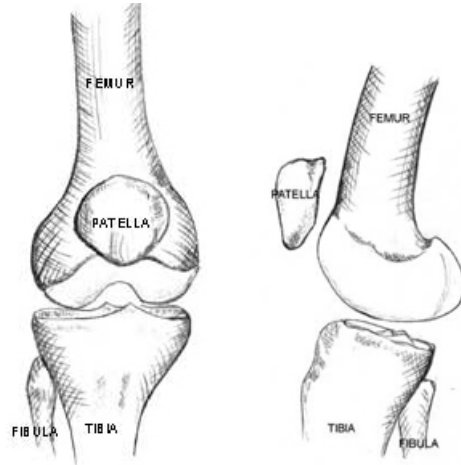


Figure 1.1: The figure illustrates the basic bone anatomy of the human knee as seen from the coronal plane (left) and from the sagittal plane (right). Observe the major bone parts femur, tibia, fibula and patella that also are visible in MR images of the knee. Image credit: Strover S, <http://www.kneeguru.co.uk>.

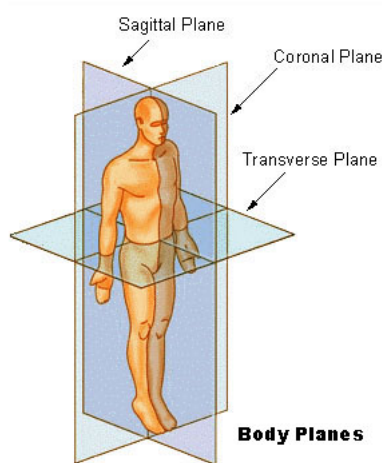


Figure 1.2: The figure shows the three reference planes from where the MRI slices are taken from. The directions are the sagittal, coronal and the transverse.

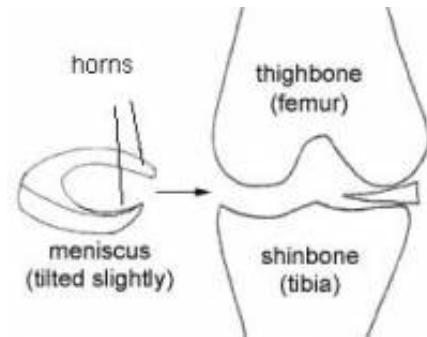


Figure 1.3: The figure illustrates the location of the menisci. The knee is shown from the frontal view and the meniscus is located at the contact surfaces between the femur and tibia. Note that each knee has two menisci, known as the lateral and medial menisci. Image credit: Strover S, <http://www.kneeguru.co.uk>.

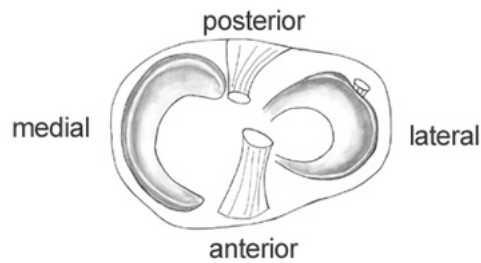


Figure 1.4: The figure shows the basic parts of the meniscus from above. Note the endpoints of the half moon shaped meniscus, on both the lateral and medial meniscus, referred to as the posterior and anterior horns. Image credit: Strover S, <http://www.kneeguru.co.uk>.

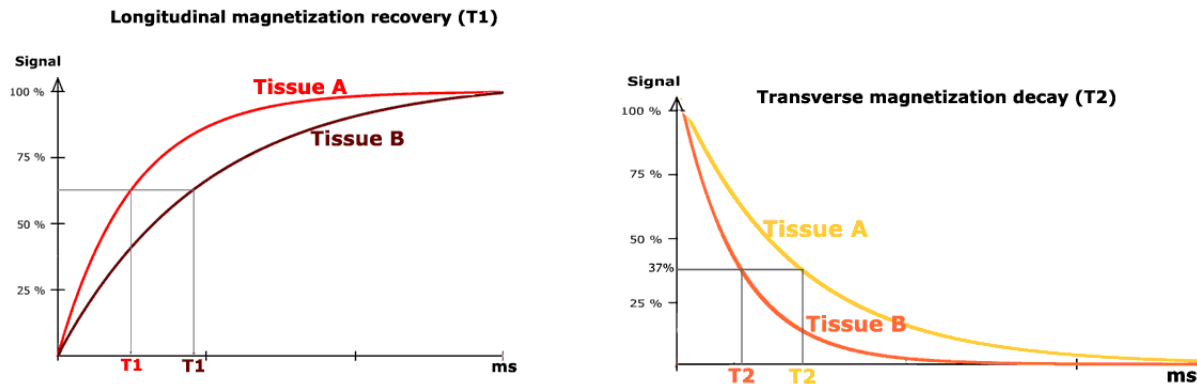


Figure 1.5: The figure illustrates how the signal depends on the tissue. The image to the left shows the signal behavior from a T1-weighted examination and the right a T2-weighted examination. Since the signal depends on the tissue the different tissue types will have different intensities in the MR image. Image credit: e-MRI, Hoa D, www.imaios.com.

the tissue to get back to equilibrium after the RF-signal and this depends on different tissue types. T1-weighted images give a weak signal for long T1 times and T2-weighted give a high signal for long T2 time, cf. [7, page 31-32], see figure 1.5. The difference in the signal strength creates an intensity difference between the different tissues in a MR image.

As previously indicated one important property is the proton density and that makes MR sensitive to water which makes up to 70-90% of most tissue. The amount of water in the tissue can alter with diseases or injury which changes the output signal compared to a healthy tissue, cf. [22, page 4]. This makes MRI an excellent tool to evaluate soft tissue, tendon, ligaments and menisci in the knee, cf. [22, page 24]. In MR, several 2D slices are produced to create a 3D object that can be visualized. In figure 1.2 the body plane with the three major directions are shown. The directions are the sagittal, coronal and transverse plane.

1.3 Image Acquisition

Images used in this Masters's thesis were produced at the hospital in Landskrona from a Philips 1,5T machine using a spin-echo sequence with repetition time 2 s, echo time 8.8 ms, matrix size 512 × 512 pixels, pixel spacing 0.28 × 0.28 mm and slice thickness 3 mm.

1.4 Related Work

This Master's thesis was first supposed to be a continuation of Klas Josephsson's Master's thesis from 2004, "Segmentation of Magnetic Resonance Images of the Knee using Three-Dimensional Active Shape Models", [12]. During this work he was able to segment the femur bone from the MR-images by using active shape models. One approach to automatically segment the menisci would be to follow up this report by adding segmentation of the tibia and patella to extract all bone present in the images. If all bone were segmented the images would be classified as less noisier and that would have been a good start in the aim to segment the menisci. However the use of shape models for segmenting the menisci was lately developed by Jurgen Fripp et al, [8]. In this report they used 3D statistical shape and thickness model based approach to first segment the bones and cartilage from the MRI, cf. [10, 9] and later they also made an segmentation of the menisci with a shape model approach on healthy knees, cf. [8]. As they concluded in the report this approach could with further work become a robust and fairly accurate method to automatically segment the menisci, however in present time this system tends to undersegment the menisci. This will of course result in volume errors between manually and automatically segmented menisci volumes.

Due to time limitation and the fact that there were complications in the starting process of making Klas Josephssons Master's thesis work correctly it was decided to try and segment the menisci with another approach. This was only based on the fact that the troubleshooting was too time consuming. This depended on the long time between the Master's theses that resulted into valid information and correct versions of the program were not found.

The request to actually segment the menisci was still valid. The new approach for this Master's thesis based on the article "An automatic diagnosis method for knee meniscus tears in MR images", cf. [14]. In this report the authors automatically locates the anterior and posterior horns in 2D MR images in the sagittal view. They used a histogram and statistical segmentation based method to locate the meniscus. The horns were then classified by using a triangular template matching. Healthy anterior and posterior horns have a known shape and look like triangles in the sagittal plane. The system is not perfect and needs a better method for locating the menisci region to increase the accuracy.

The third and last report that included an automatic segmentation of the menisci was found in the process to discriminate normal and degenerated menisci with texture analysis, cf. [3]. In this report the authors constructed a program to automatically segment the posterior horns of the medial meniscus with a region growing segmentation approach. As the previous article these systems are used to segment the menisci horns and not the whole menisci.

Two articles describing semiautomatical systems were found. The first system, cf. [11], included several manual steps and used the interference between T1-weighted and T2-weighted images with fuzzy interference. This system segmented the menisci and then provided a 3D surface that could be used for assisting when diagnosing meniscal tears. The second article, cf. [20], tries to segment the lateral meniscus in normal and osteoarthritic knees with a method based on

thresholding and morphological operations. This system needs some manually steps and the segmentation result is not always that accurate.

Chapter 2

Theory

2.1 Laws' Texture Algorithm

Texture analysis is used in several areas such as classification and segmentation problems. Textures are various patterns in images. Identifying these patterns is a result of extracting features from patterns in different images. In 1979 K.I Laws proposed a texture energy approach, cf. [19], that classifies each pixel by extracting features. The method estimates the energy inside a region of interest by energy transformation. The transformation only requires convolution and a moving window technique. Laws' developed a two-dimensional set of filter masks that was derived from five one-dimensional filters. The set is used to detect features from patterns. Each one-dimensional filter vector was constructed to detect different microstructure in the images. Microstructure of interest are level detection, edge detection, spot detection, wave detection and ripple detection, cf. [18, 16, 17, 19].

$$\begin{aligned} \text{Level detection:} & \quad L_5 = [1 \ 4 \ 6 \ 4 \ 1]. \\ \text{Edge detection:} & \quad E_5 = [-1 \ -2 \ 0 \ 2 \ 1]. \\ \text{Spot detection:} & \quad S_5 = [-1 \ 0 \ 2 \ 0 \ -1]. \\ \text{Ripple detection:} & \quad R_5 = [1 \ -4 \ 6 \ -4 \ 1]. \\ \text{Wave detection:} & \quad W_5 = [-1 \ 2 \ 0 \ -2 \ -1]. \end{aligned}$$

From these one dimensional vectors 25 two-dimensional masks \mathbf{m} of size 5×5 were created by convolution between all possible combinations of these vectors and their transpose. 24 of these masks are zero-sum but the $\mathbf{m}_{L_5 L_5}$ is not. The result is referred to as \mathbf{m}_l , where l indicates which of these masks that is used,

$$\begin{array}{ccccc} L_5^T L_5 & L_5^T E_5 & L_5^T S_5 & L_5^T R_5 & L_5^T W_5 \\ E_5^T L_5 & E_5^T E_5 & E_5^T S_5 & E_5^T R_5 & E_5^T W_5 \\ S_5^T L_5 & S_5^T E_5 & S_5^T S_5 & S_5^T R_5 & S_5^T W_5 \\ R_5^T L_5 & R_5^T E_5 & R_5^T S_5 & R_5^T R_5 & R_5^T W_5 \\ W_5^T L_5 & W_5^T E_5 & W_5^T S_5 & W_5^T R_5 & W_5^T W_5 \end{array}$$

The approach to extract features with Laws' texture algorithm in this Master's thesis is divided into three parts:

- 1: Construct the different masks.
- 2: Construct energy measurement.
- 3: Calculate features from energy measurements.

First the image $I(i, j)$ of size $r \times c$ needs some preprocessing before it is ready to be analyzed. Images to be analyzed with Laws' texture in this thesis all have the same size of 5×5 pixels. The purpose of the preprocessing is to erase the mean intensity of the image and keep the interesting parts of the image,

$$f = I - \frac{\sum_{i=1}^r \sum_{j=1}^c I(i, j)}{r \cdot c}. \quad (2.1)$$

This will give a better picture of how the environment or in this case the textures randomness looks like. This new image will be convoluted with each of the masks,

$$TI_l = f * m_l. \quad (2.2)$$

Each texture image, TI_l , will be normalized with the L_5L_5 mask since this mask had not zero mean as discussed earlier. The texture energy measurements, TEM , will be calculated by moving a window in the normalized images. The window summarizes the absolute value in a neighborhood of 5×5 pixels. This will create a new set of 25 images of size 5×5 pixels known as TEM. Note that the image size of the TI_l was 9×9 pixels i.e. the image sizes are back to the original sizes after this texture energy measurement,

$$TEM_l(i, j) = \sum_{m=i-2}^{i+2} \sum_{n=j-2}^{j+2} |TI_l(m, n)|. \quad (2.3)$$

By combining similar features with each other a set of 14 new images is created,

$$TR_{X5Y5} = \frac{TEM_{X5Y5} + TEM_{Y5X5}}{2}, \quad (2.4)$$

where X5Y5 indicates which of the masks that is added to each other. For instance a single image that is sensitive to edges, $TR_{E_5L_5}$, is created by adding the $TEM_{E_5L_5}$ with the $TEM_{L_5E_5}$, where $TEM_{E_5L_5}$ is sensitive to the horizontal edges and the $TEM_{L_5E_5}$ is sensitive to the vertical edges.

The final 14 images are,

$$\begin{array}{ccccc} TR_{E_5E_5} & TR_{E_5L_5} & TR_{E_5S_5} & TR_{E_5R_5} & TR_{E_5W_5} \\ TR_{L_5S_5} & TR_{L_5R_5} & TR_{L_5W_5} & TR_{S_5S_5} & TR_{S_5R_5} \\ TR_{S_5W_5} & TR_{R_5R_5} & TR_{R_5W_5} & TR_{W_5W_5} & \end{array}$$

Features used in this thesis are extracted from these 14 images. From each image five features are calculated. The features are mean intensity, standard deviation, entropy, skewness and kurtosis. One additional feature is added and that is the mean intensity from the original image. This implies that 71 features are calculated to each image that is being analyzed .

2.2 Graph Cut

Graph cuts is a well known method for image segmentation. The image is optimally divided into two parts by calculating the min-cut between the segments known as the foreground and background.

A graph $G(V, E)$ consists of a collection of nodes, or vertices (V), and a collection of edges (E) that connect the vertices with nonnegative weights w_e . In an image all pixels will be represented as a vertex and the edges are the links between the neighboring pixels. Two additional vertices are connected to each pixel, also known as the terminal nodes and they represent the foreground/background labeling. The first terminal node is referred to as source, s , and represents the foreground. The other terminal is known as sink, t , and represents the background. Edges are often divided in two parts. The first part, n -links, connects pairs of neighboring vertices. An edge connects two vertices and the cost will be weighted depending on the similarity between the pixel and its surrounding. In 2D the neighborhood consists of the 4 or 8 closest vertices. The second part, t -link, connects the vertices with the terminals. This means that the cost between the vertex and the terminal corresponds to the penalty for assigning the vertex to that specific terminal.

The image in the left column in figure 2.1 illustrates an image of 3×3 pixels. As said before each vertex is connected to the terminal nodes s and t as seen in the image in the middle column, t -link. The image in the right column shows how the pixels are connected to each other, n -link. In this example the pixels are connected to the four closest pixels.

A cut is to separate the vertices in two disjoint subsets, S and T , so that no paths from the terminal nodes s and t exist to each other. In other words $s \in S$, $t \in T$, $S \subset V$ and $T \subset V$. The cut can be performed in many ways, however there will always be a cut that have the minimum cost, i.e. min-cut. Figure 2.2 illustrates a cut in the image of 3×3 pixels where the subset connected to the source (s) is called the foreground and the subset connected to the sink(t) is called the background.

In this Master's thesis the implementation of graph cut algorithm by Boykov and Kolmogorov is used to calculate the min-cut or max-flow [5]. This min-cut/max flow can be calculated by minimizing the discrete approximation to the energy function,

$$E(\gamma) = \underbrace{\lambda \text{length}(\gamma)}_{\text{regularization term}} + \underbrace{\int \int_{\Gamma} (I(\mathbf{x}) - \mu_1)^2 d\mathbf{x} + \int \int_{\Omega/\Gamma} (I(\mathbf{x}) - \mu_0)^2 d\mathbf{x}}_{\text{data terms}}, \quad (2.5)$$

where I is the image and the foreground and background are modeled as having a constant intensity, μ_0 and μ_1 respectively. The segmentation problem involves finding a curve γ that minimizes the energy $E(\gamma)$ so that the region inside Γ is labeled as foreground and the remaining parts are labeled as background, see

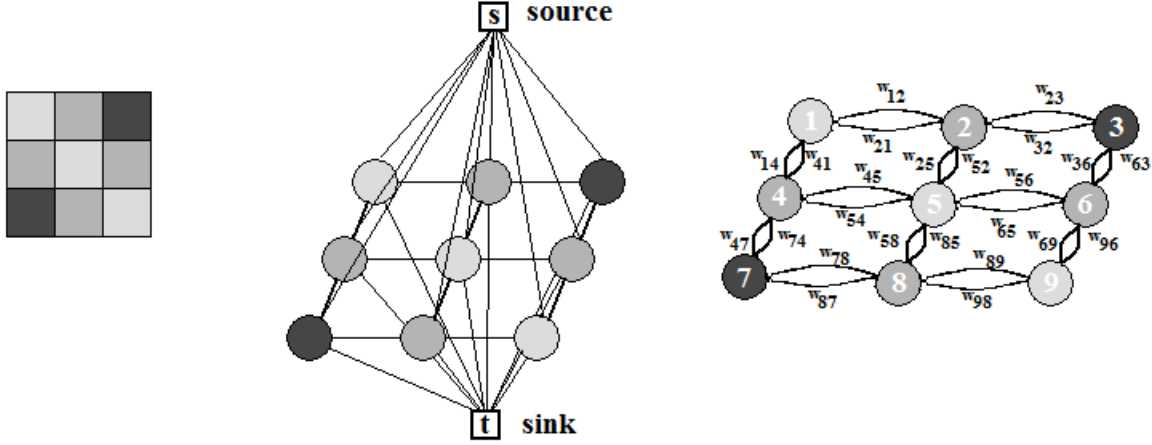


Figure 2.1: The image in the left column illustrates an image of 3×3 pixels and will be used in these examples. Each pixel or vertices is connected to the terminal nodes called s (source) and t (sink) as shown in the middle column. This is known as the t -link. The right column shows the edge connection between the neighboring pixels, known as the n -link. In this case the neighborhood consist of the four closest vertices. The cost w_e between the vertices depends on the similarity between the pixels.

figure 2.3. Equation 2.5 is approximated to a discrete problem,

$$E(f) = \underbrace{\sum_{p \in P, q \in N_p} V_{p,q}(f_p, f_q)}_{\text{regularization terms}} + \underbrace{\sum_{p \in P} D_p(f_p)}_{\text{data terms}}. \quad (2.6)$$

where N_p is a set of pixels in the neighborhood of p . If pixel p is connected to pixel q then $q \in N_p$. If the pixel p belongs to the foreground, $p \in S$ the pixel is labeled $f_p = 1$. If the pixel p belongs to the background $p \in T$ the pixel is labeled $f_p = 0$.

The energy function E contains two parts, D_p and V_{pq} . D_p is called the data term and represents the penalty for assigning the pixel to the label i.e. either the foreground or background,

$$D_p(f_p) = \begin{cases} (I_p - \mu_0)^2 & \text{if } f_p = 1 \\ (I_p - \mu_1)^2 & \text{if } f_p = 0 \end{cases}. \quad (2.7)$$

where I_p is the intensity of pixel p , μ_0 is the modeled mean intensity of the foreground and μ_1 is the modeled intensity of the background. V_{pq} is known as the interactive term or regularization term that is influenced by the variation in

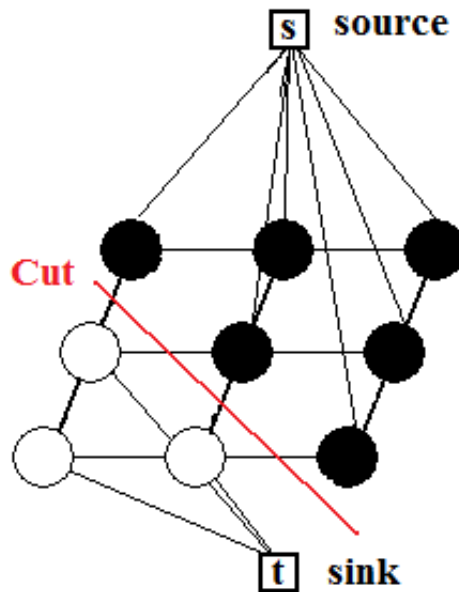


Figure 2.2: A cut is to separate the vertices in two disjoint subsets, S and T, so that no paths from the terminal nodes s and t exist.

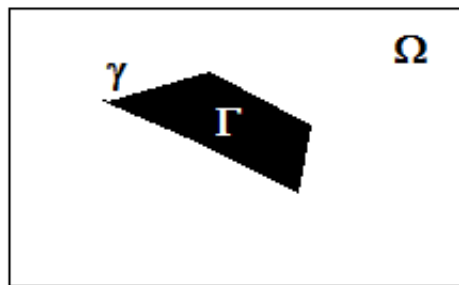


Figure 2.3: This figure illustrates a segmented image where the region Γ indicates the foreground with the curve γ describing the boarder.

a given neighborhood of the pixel,

$$V_{p,q}(f_p, f_q) = \begin{cases} 0 & \text{if } f_p = f_q \\ \alpha & \text{if } f_p \neq f_q \end{cases} . \quad (2.8)$$

where

$$\alpha = \exp\left(-\frac{(I_p - I_q)^2}{2\sigma^2} \cdot \frac{1}{\text{dist}(p, q)}\right). \quad (2.9)$$

I_p and I_q is the intensity of the pixel p and q in the image, σ is the standard deviation of the intensity in the image and $\text{dist}(p, q)$ is the Euclidian distance between pixel p and q . For more information regarding graph cuts, cf. [4, 13].

Chapter 3

Segmentation Workflow

The overall approach for segmentation of the menisci is explained in this chapter.

Figure 3.1 shows four MR images taken from the sagittal view. In this figure the meniscus has been manually segmented to clarify its location. The MR image is considerable bigger than the meniscus and contains much information about other areas. However, most of this information is not of interest and will be classified as noise since it disturbs the segmentation process. Note the intensity similarity and undefined borders between the different tissue and bone parts in the figure. The overall approach is shown in figure 3.2, but the three major parts to segmenting the menisci are:

- 1: Segmentation of bone in the MR images.
- 2: Localize the area where the menisci can be found.
- 3: Segmentation of the menisci.

In this report only information from the sagittal plane will be used since the characteristic triangular shape of the posterior and anterior horns of the meniscus can be found in this view.

3.1 Segmentation of Bone

The main idea with segmentation of bone in the images is to find features that will characterize the pixels as either bone or not bone. Features are extracted with Laws' texture algorithm, discussed in section 2.1. The segmentation process starts with manually creating a database with features from known texture parts. The database is refereed to as classdata and consist of features extracted from smaller areas of either bone or not bone. During the actual segmentation process features will be extracted from smaller areas of the image and later compared to the classdata. This classification calculates a probability that the area is either bone or not bone.

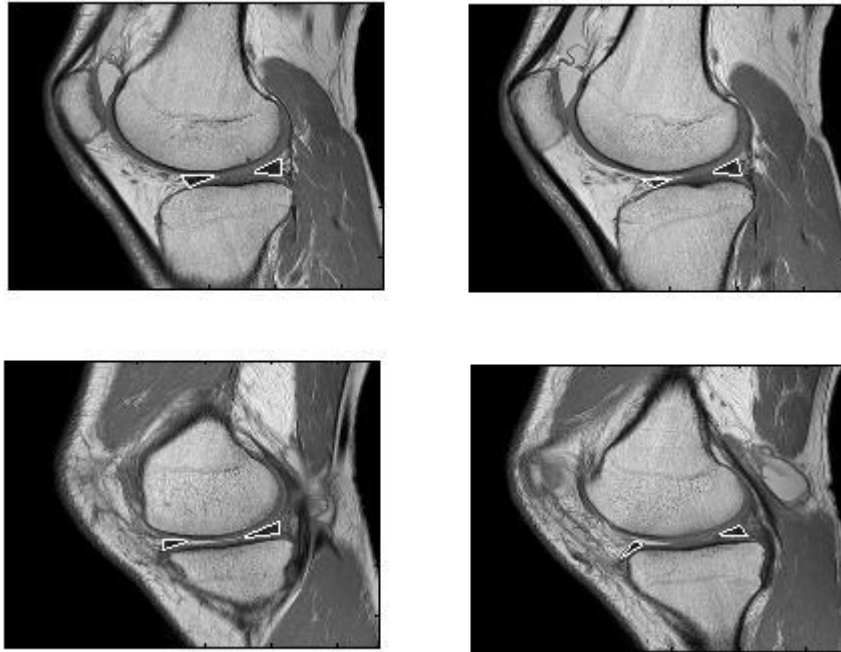


Figure 3.1: The figure shows four MR images from one examination from four different slices in the sagittal plane. In these images the meniscus is manually segmented with white marks to show the location and the difficulties of segmenting it. The meniscus is very small compared to all the other information present in the image. One major noise problem is the presence of bone. All three major bone parts discussed earlier in figure 1.1, femur, tibia and patella are present in the images.

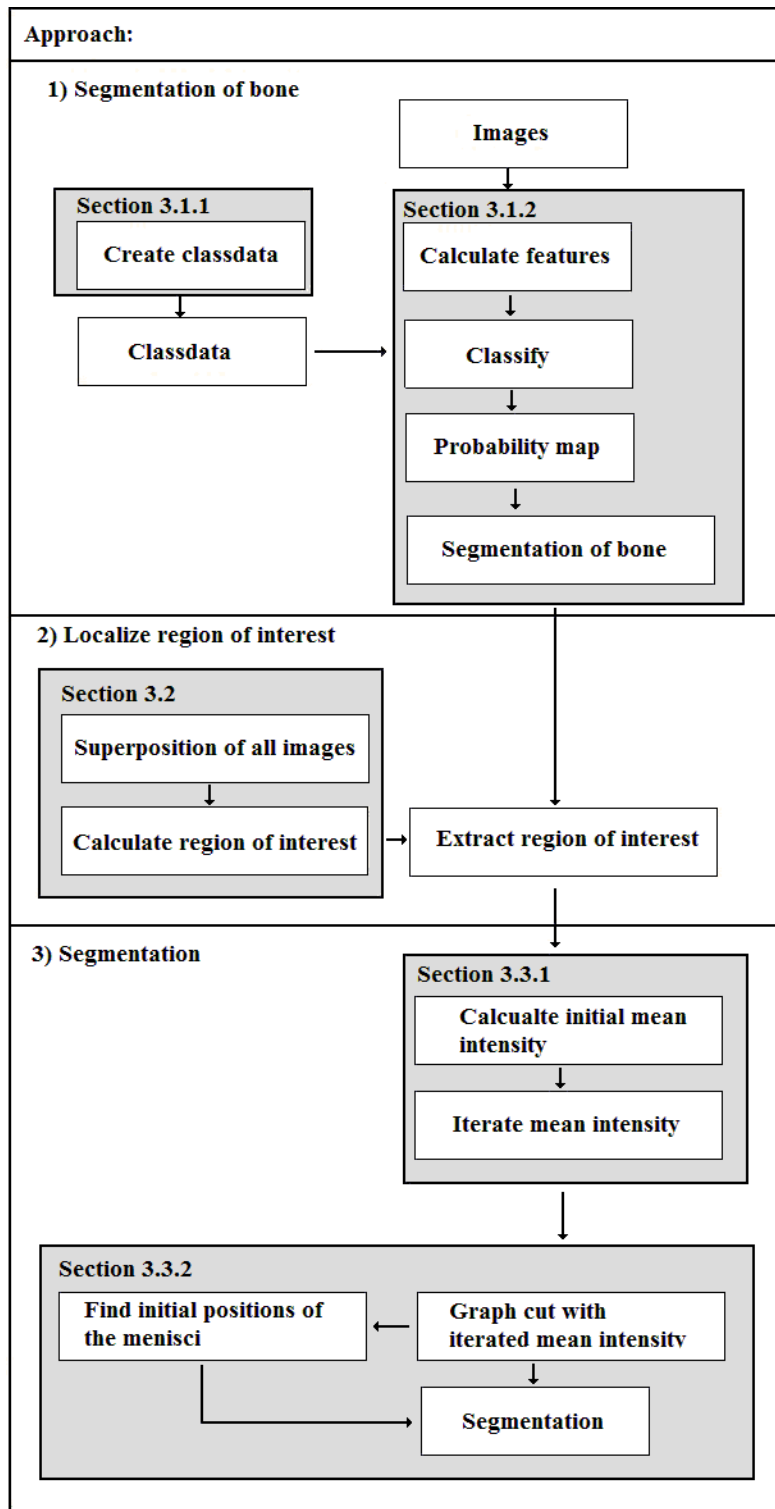


Figure 3.2: This figure illustrates the main segmentation workflow.

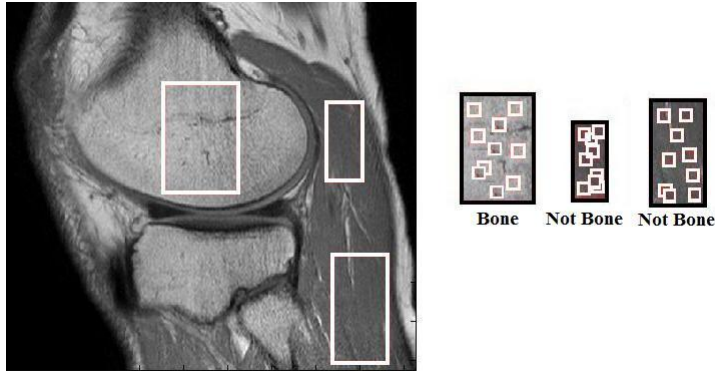


Figure 3.3: The image to the left shows three manually selected regions in a MR image. From each region 10 smaller areas of size 5×5 at random positions are extracted(right image). The smaller areas are then used to extract features with Laws' texture algorithm. This means that a database is created by calculating features from areas that are manually classified as either bone or not bone. The database is referred to as classdata.

3.1.1 Create Classdata with Laws' Texture Algorithm

In the given MR images textures as tissue, bone, cartilage are visible and they all have different texture properties. The purpose of creating classdata is to build a database with extracted features from different classes, either bone or not bone. At this moment the main purpose is to segment the major bone parts in the images. This means that the system does not separate different tissues, they will only be classified as bone or not bone. The features are extracted with Laws' texture algorithm discussed in section 2.1. To construct this database the user has to manually select different region of interest (ROI) in several images. Each RIO is also labeled as either bone or not bone. When the user manually selects a ROI in the image the program automatically selects 10 random areas by the size of 5×5 pixels and extracts features from these sub images, as illustrated in figure 3.3.

3.1.2 Segmentation Process for Segmenting Bone With Graph Cut

This section describes how to use the created classdata to analyze the MR images from an examination. The workflow for automatically segmenting the bone is:

- 1: Calculate features with Laws' texture algorithm.
- 2: Classify the texture with k-nearest neighbor.
- 3: Create a probability map.

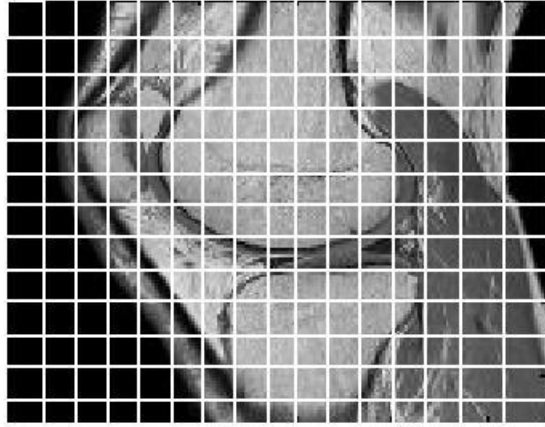


Figure 3.4: This figure illustrates how smaller sub images are extracted from one image. The sub images are 5×5 pixels big and are used to calculate features. The features are then compared to the classdata.

4: Segment bone with graph cut.

The essential difference when calculating features in the segmentation process compared to creating the classdata is that during this process no areas are manually selected. The process starts with creating sub images of size 5×5 pixels. The sub images are created by dividing the entire image in sub images of size 5×5 with no overlap. This implies that sub images are extracted from the entire image, see figure 3.4.

Features are then calculated from each sub image with Laws' texture algorithm. Each feature vector \mathbf{v} from the sub image are then compared to the feature vectors \mathbf{w} from the classdata with k-nearest neighbor classification. This classification calculates the Euclidian distance between the two vectors

$$d(\mathbf{v}, \mathbf{w}) = \sqrt{\sum_{i=1}^n (v_i - w_i)^2}, \quad (3.1)$$

where n is the total number of feature vectors in classdata.

By saving the 16 best results from the classification in a vector a probability classification may be calculated. The vector contains how many of the 16 best results that were classified as bone. A probability map, P , was calculated by comparing how many of the 16 best results that were classified as bone. The probability map is a binary map of the same size as the image that is being

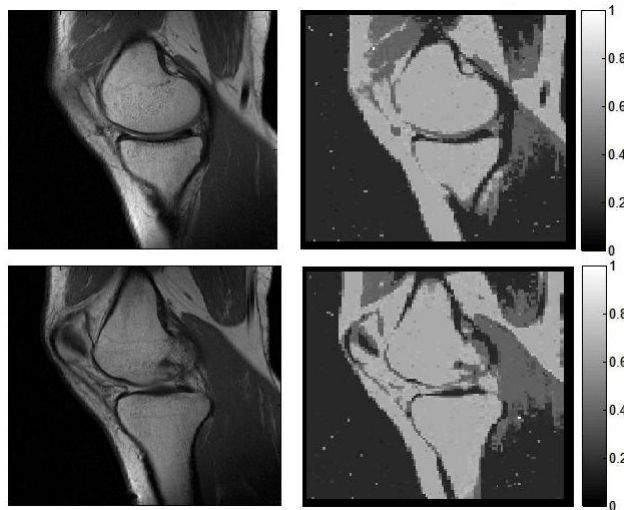


Figure 3.5: In the left column, the original MR images are shown. The right column shows the probability map constructed in the classification process. Observe that the probability map is created from the certainty that the extracted sub image is bone. Brighter areas indicates that the system is more certain that the sub images are bone.

analyzed. The pixel intensity is therefore represented as the probability of being bone, $P \in [0, 1]$. If the system is confident that the sub image is not bone a zero is generated at the sub image location. If the system is confident that the sub image is bone a one is generated. Figure 3.5 shows the probability map from two images. The left images illustrate the original MR image and the right images show the result from the classification process. This probability map is then used to localize the bone by using graph cuts. Using graph cut will classify the image pixels as bone or not bone by calculating the min-cut of the probability map. This is a binary segmentation and will divide the image into two classes. As discussed earlier, see section 2.2, the two classes will be represented as either foreground(bone) or background(not bone). The foreground mean intensity is determined by calculating the mean intensity from the original image from those pixels that were classified as bone, i.e. pixels that have higher intensity than 0.5 in the probability map. The background mean intensity is calculated with the same procedure, but the localized pixels in the probability map have an intensity lower than 0.5.

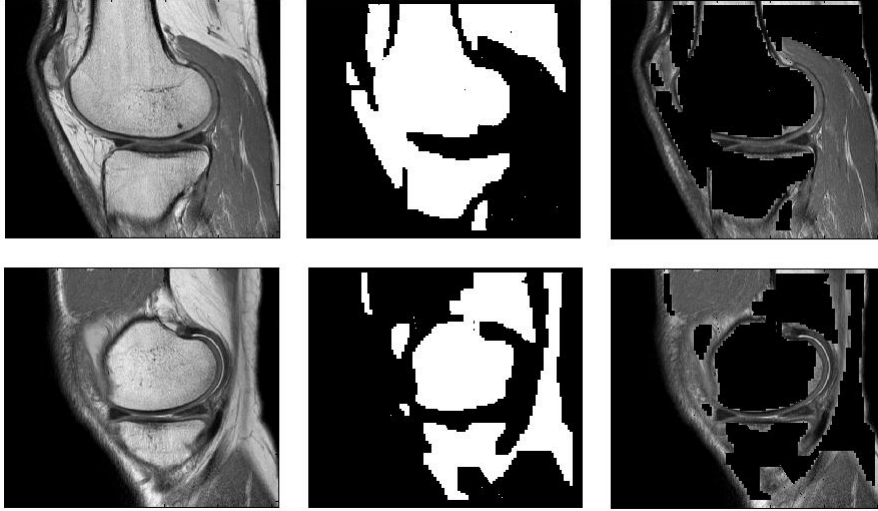


Figure 3.6: This figure contains two examples from bone segmentation with the described method. The images in the left column are the original MR images. In the middle column the result from the graph cut method is shown. White pixels indicate the foreground i.e. bone. The images in the right column show the result when extracting the bone parts from the original images.

$$\mu_{\text{bone}} = \frac{\sum_{i=1}^r \sum_{j=1}^c I(i, j) \cdot z_{\text{bone}}(i, j)}{\sum_{i=1}^r \sum_{j=1}^c z_{\text{bone}}(i, j)}, \quad z_{\text{bone}} = P \geq 0.5, \quad (3.2)$$

$$\mu_{\text{bone}} = \frac{\sum_{i=1}^r \sum_{j=1}^c I(i, j) \cdot z_{\text{notBone}}(i, j)}{\sum_{i=1}^r \sum_{j=1}^c z_{\text{notBone}}(i, j)}, \quad z_{\text{notBone}} = P < 0.5,$$

where μ is the calculated mean intensity from the image I , with the size $r \times c$, at the pixel locations determined by z . The threshold value of 0.5 is determined in section 4.1. During the graph cut segmentation one adjustment needs to be done. To get a more accurate and smoother cut around the bone edges around femur and tibia an edge detection is used. The pixels that are detected as edges with this method receive a low cost. Two examples from the bone segmentation can be seen in figure 3.6. The images in the left column show the original MR images, and the images in the middle column show the graph cut min-cut where the white pixels are known as the bone parts. The last images in the right column show the result after removing the segmented bone parts from the original images.



Figure 3.7: The image to the left illustrates the result when all images are added to each other, via superposition, to one image. By using a thresholding and histograms based method the menisci area can be found so that the size of the MR images are reduced which results in less noise in the images. The middle image shows the result after thresholding the left image. The right image shows the area of where the menisci should be located and this area is used to reduce the image size.

3.2 Find the Correct Localization of the Menisci

Even if the bone is segmented the image still contains a lot of noise. One big issue is the image size. The meniscus is very small compared to the entire image, but before the image size can be reduced the menisci have to be found. In the article by Kose, C.; Gencalioglu, O.; Sevik, U [14] they try to use a histogram based method to find the menisci. The bone gap between the femur and tibia results in a good initial estimation for the vertical position, but the horizontal position was harder to localize.

Taking this into consideration and using the geometry of the bone, the menisci area was found by sampling the segmented bone images to each other. Using this superposition system an image was created based on how often each pixel was classified as bone, see figure 3.7. As described in section 1.1 the menisci are located between the surfaces of the femur and tibia bones. The menisci area can therefore be found by locating those pixels that often recur as bone i.e. have a high intensity value in the superposition image. The middle figure shows the superposition image after thresholding. The right figure shows the superpositioned image as well as the menisci area of where the menisci should be located. The area is found by a thresholding and histograms based algorithm of the superposition image.

3.3 Segmentation of the Menisci

When the menisci area was located much smaller images could be extracted. This reduces the noise in the image. Even if the new image reduced the noise the problem of segmenting the menisci still exists. The method for segmenting the menisci is divided into two parts. First the mean intensity of the menisci had to

be found. The mean intensity of the menisci was then used in the segmentation process with graph cuts in the second part.

3.3.1 Finding the Mean Intensities of the Meniscus

At this moment all that is known is that the menisci are located somewhere in the new image defined by the menisci area. Where and what it looks like are unknown. The segmentation process with graph cut method needs to know the mean intensity of both the foreground and background. The foreground in the segmentation process will be the mean intensity of the located meniscus and the background will be the mean intensity of the new image. The workflow for finding the mean intensity of the meniscus is:

- 1: Calculate features with Laws' texture algorithm.
- 2: Create a probability map with k-nearest neighbor classification.
- 3: Create a binary image of the probability map with graph cut.
- 4: Find an initial mean intensity with triangular template matching.
- 5: Use graph cut to iterate a converged mean intensity.

The first three steps use the same process as the segmentation of bone. For more details, see section 3.1. The initial step is to create a database with features, calculated from Laws' texture algorithm, from areas known as meniscus or not meniscus. Note that the pixels classified as bone are segmented in these images. Each image is divided into sub images of size 5×5 pixels, see figure 3.4. Texture features are extracted from each of these sub images with Laws' texture algorithm. These features are then used to create a probability map by comparing the features from each sub image with the database using k-nearest neighbor classification. The left column in figure 3.8 shows the located menisci area for two slices in one examination. Black areas in this image are the extracted bone segments that were previously segmented in section 3.1. The probability map is shown in the middle column. The probability map, $P \in [0, 1]$, shows how certain the system is that this specific area in the sub image is menisci parts. The right column shows the result of the graph cut method used on the probability map. Like before, the meniscus mean intensity is determined by calculating the average of the pixel intensities that is classified as meniscus i.e. pixel intensities higher than 0.5, and vice versa for the not meniscus mean intensity, see equation 3.2. Note that this graph cut segmentation is not optimized and not very accurate, compare the left and right images in figure 3.8.

To improve the systems segmentation accuracy the mean intensity of the meniscus had to be optimized. The foreground from the graph cut method represents parts of the meniscus and cartilage. To find the initial mean intensity μ_{initial} of the meniscus a template search method is used on the previous result from the graph cut segmentation.

- 4.a: Save the 20 best matches between the previous graph cut images and the templates. Also save their coordinates by calculating the center of mass between the images and the templates.
- 4.b: Determine the mean intensities in the close neighborhood from these coordinates.
- 4.c: Find the initial mean intensity in a histogram from the 20 saved mean intensities.

The result from the graph cut on the probability map was a binary image that contained two labels, meniscus and not meniscus. The meniscus part in this case contains parts of the menisci and cartilage. A template search method is used to search for the meniscus posterior horns in the image by moving the template around the image. As discussed earlier the horns have a characteristic shape as triangles in the sagittal plane. These shapes were used to create templates of how the meniscus horns might look like. The shape reconstruction was created with principal component analysis, PCA, for more details see [1, page 507-509]. Each shape reconstruction was then used with several angle rotations in the template search model. The template search method compares the intensity of the image where the objects are searched for and the template. Since the image and the templates only are binary images of zeros and ones the search method will measure how well the template matches the sub region in the image,

$$M(x, y) = \sum_{i=0}^{T_{rows}} \sum_{j=0}^{T_{col}} |I(x+i, y+j) - T(i, j)|, \quad (3.3)$$

where T_{rows} and T_{col} is the image size of the template T . I is the image and M is the cost from the template match. From the 20 best matches the mean intensity is calculated. Each match corresponds to a coordinate calculated by the center of mass between the image and the template

$$\mathbf{R} = \frac{\sum m_i \mathbf{r}_i}{\sum m_i}, \quad (3.4)$$

where \mathbf{R} is the coordinates for the center of mass, \mathbf{r} is the position of the concerned pixels and m is their weight. The mean intensity is calculated by determining the average mean intensity in a close neighborhood from these coordinates. A new mean intensity $\mu_{menisci}$ was then created by searching for the most common intensity in a histogram constructed from the mean intensities.

To refine the mean intensity of the meniscus an iterative approach was used.

- 5.a: Use graph cut method with the calculated mean intensity.
- 5.b: Remove big objects with morphological operations. Objects that were removed are saved in a morphological map.
- 5.c: Search for the meniscus with a triangular template method to find the mean intensity.

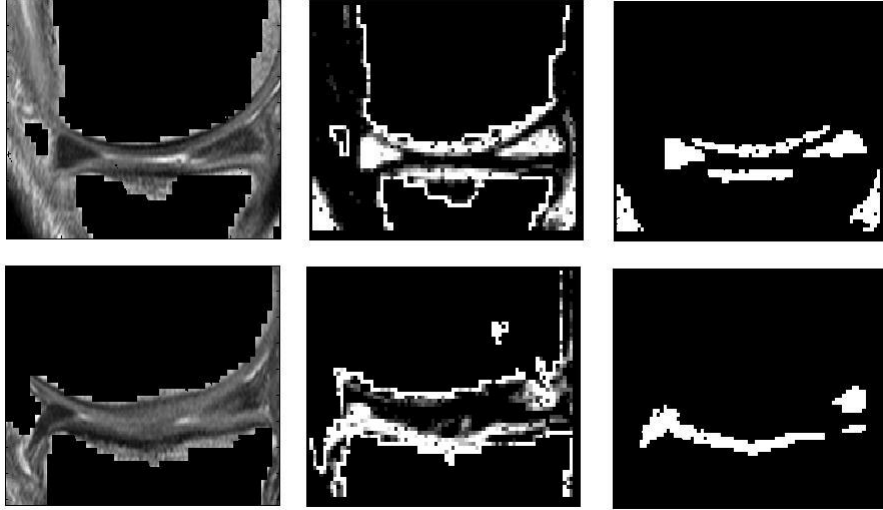


Figure 3.8: The images in the left column show the reduced size of the MR image. Also observe that the bone is segmented. In the middle column the probability map, $P \in [0, 1]$, is shown. The intensity is proportional to how certain the system is that the pixels are a piece of the meniscus. The right column shows the result from the graph cut process.

5.d: Return to 5.a with an updated mean intensity and morphological map if the intensity has not converged.

First the graph cut method is used with the initial mean intensity of the meniscus. To get a better initial guess of the mean intensity bigger objects was removed with morphological operations. If some objects were removed the positions were saved in a binary image called morphological map, $M \in [0, 1]$. Next step is to search for the meniscus posterior and anterior horns in the image with the template search method discussed earlier in this section. An iterative process was then used to search for a mean intensity that converges. If the mean intensity is not inside a tolerance limit t ,

$$\mu_{\text{converged}} = |\mu_{\text{menisci}} - \mu_{\text{initial}}| < t, \quad (3.5)$$

the graph cut method is used with the new mean intensity, $\mu_{\text{initial}} = \mu_{\text{menisci}}$, with the change that located big objects in the morphological map receive a high cost of being a meniscus part in the graph cut segmentation process. This process continues until the intensity converges.

3.3.2 Segmentation Process

The segmentation process is based on using a 2D graph cut while using information from the nearest images. Segmentation of the meniscus is a difficult problem

since the soft tissue sometimes can be very similar and has undefined borders. The segmentation process is divided in three parts:

- 1: Use the graph cut method with the converged meniscus intensity.
- 2: Find the initial positions of the posterior and anterior horns of the lateral and medial menisci.
- 3: Use graph cut to segment the menisci.
- 4: Extract the menisci parts to create a 3D model.

Even if the images have been substantially reduced in image size the only known fact is that the menisci are located somewhere in the region defined as menisci area. Therefore it is crucial to find some part of the menisci in the image set. The image set contains all images from one examination in the sagittal view. The list below describes the necessary parts for locating the initial position.

- 2.a: Use graph cut method with the converged mean intensity.
- 2.b: Filter big objects in the images with morphological operations.
- 2.c: Use superposition and thresholding to refine the menisci search area.
- 2.d: Find the initial position of the anterior and posterior horns on both the lateral and medial menisci using triangular template search method.

Finding the initial positions of the posterior and anterior horns is based on the fact that the horns have a triangular shape. A triangular template method is used to localize the best match of both the lateral and medial menisci. The image set contains images of the entire knee including the lateral and medial menisci. However, the images contain a great deal of noise that influence the template search method. Noise in this case represents other soft tissue as e.g. cartilage around bone surfaces. Some of these objects give a very good match in the template search method, resulting in poor initial position guesses for the menisci. This is the reason why the image set needs to be filtered to reduce the noise. First all big objects are removed with morphological operations. After this operation mostly soft tissue between the femur and tibia is displayed. By implementing a superposition method that uses thresholding and histograms to locate a reduced region of interest the noise is decreased. The left image in figure 3.9 illustrates the image from the superposition. The area found from the thresholding and histogram based method is shown in the right image. From this image a refined search area is found by only searching in a limited neighborhood of the found objects. This is illustrated in figure 3.10 where the left images show the result from the graph cut method with converged mean intensity, while the right images show the new refined search area that is used when searching for an initial guess of the menisci positions.

Since there are two menisci present in each set of images the set is divided in two parts, assuming that the lateral and medial menisci are present in one part each.

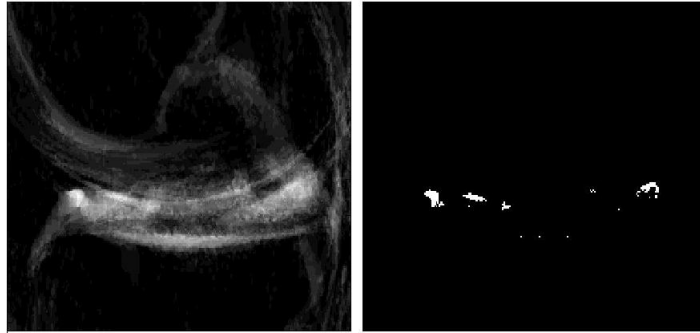


Figure 3.9: A superposition of all images is used to refine the search area for locating the initial positions of the lateral and medial meniscus. To the left the result of the superpositioned images are shown. The intensity is based on how often the pixel position is classified as meniscus from the previous graph cut method. By thresholding these superpositioned images the most common pixel locations are located (right image). This method is used to localize the vertical position which is used to refine the search area when searching for the initial position of the meniscus.

One part is the images of the medial meniscus and the other part is containing images of the lateral meniscus.

To locate the initial positions of the posterior and anterior horns a triangular template search method is implemented. A template search method was used to locate the best match to the anterior and posterior horns. This is done by assuming that the anterior horn is located somewhere to the left in the image and the posterior horns somewhere to the right. The image with the best match of both the posterior and anterior horns, as well as the initial positions of the horns are saved. The initial position of the horns are calculated by taking the center of mass of the overlapping pixels between the image and the template,

The initial positions contain information about the positions of the anterior and posterior horns of both the lateral and medial menisci in the 3D. This means that the image slice and the 2D coordinates for the menisci horns are known.

An overview of the segmentation process is given in the list below and in figure 3.11:

- 3.a: Use graph cut method with the converged mean intensity.
- 3.b: Extract the meniscus parts in the image using the initial positions.
- 3.c: Use the extracted meniscus parts to create a background map.
- 3.d: Use graph cut with the converged mean intensity and background map in the nearby images.
- 3.e: Update the initial positions of the meniscus in the nearby images.

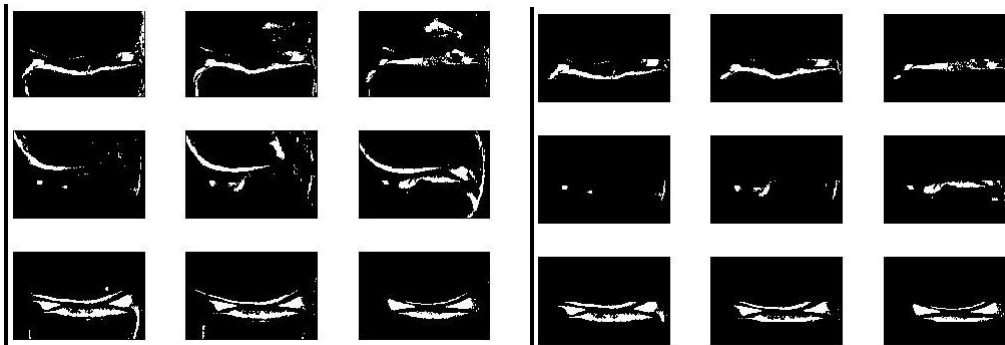


Figure 3.10: The left figure includes nine segmentation results from nine different slices from the graph cut method with converged menisci mean intensity. These images contain noise such as cartilage around the femur and tibia. The noise will interrupt the localization of the initial positions of the menisci. That is why the images are filtered with a thresholding and histogram based method, see figure 3.9. The new search area is displayed in the right figure. Even if some noise is present the filter function will make the initial guess method more robust.

3.f: Return to 3.b until all images have been used.

The images of both the lateral and the medial menisci contain noise, which disturb the segmentation process. Therefore the segmentation process needs to gather information from the nearby images. Spacial distribution between the images is very small, 3 mm in the examinations used in this work. This means that the probability of finding the neighboring parts of the meniscus in the nearby images is very high just by using the known meniscus position.

Figure 3.11 illustrates the segmentation process. The two images that gave the best match in the triangular template search are used as an initial image in the segmentation process i.e. the best initial guess for both the medial and lateral menisci. From this image the objects that interfered with the known initial positions are extracted creating an image known as the menisci image I_M . The rest of the image is used as a background map. This map is used in the graph cut method in the neighboring images. Objects in the background map will receive a high cost for being a meniscus part in the graph cut method. This will lower the noise present in the images, in this case mostly cartilage.

The initial position is calculated for one specific image and can not be used in all the other images. Therefore images created from the graph cut method are compared against the menisci image I_M in the previous slice. Objects that interfere between these images are used to create the menisci image for the new slice. The remaining objects are used to create a new background image. This process continues until all slices has been analyzed i.e. in all four directions, see figure 3.12. As explained before the initial position contains the best match for both the lateral and medial menisci. From each image this process is adapted

to the first or last image slice (depending on which is closest) and to the other initial position i.e. the segmentation process will generate two image sets.

From these four directions the menisci parts are extracted to create a visual 3D object of the menisci. The problem of extracting these menisci parts lies in that two image sets are present, and to decide which of the images to use when creating the 3D object. As described earlier this segmentation process uses interference between the graph cut images to decide what parts in the image that is classified as menisci. This implies that the initial position guess from one of the meniscuses is needed to extract the menisci parts of that meniscus. From that point of view both of the initial positions are used to extract the menisci parts outwards from that starting point. However, the problem lies in determining which of the images from the two image sets to use when extracting the menisci parts between the initial positions. When searching inwards the menisci horns in the images are located and extracted. The problem lies in finding the endpoints of the anterior and posterior menisci parts. Either the endpoints are found when the search process can not find any menisci parts or it ends when the search process finds the anterior or posterior ligaments. As seen in figure 1.4 the anterior and posterior cruciate ligament are located between the medial and lateral menisci. In figure 4.4 the result from five examinations are presented.

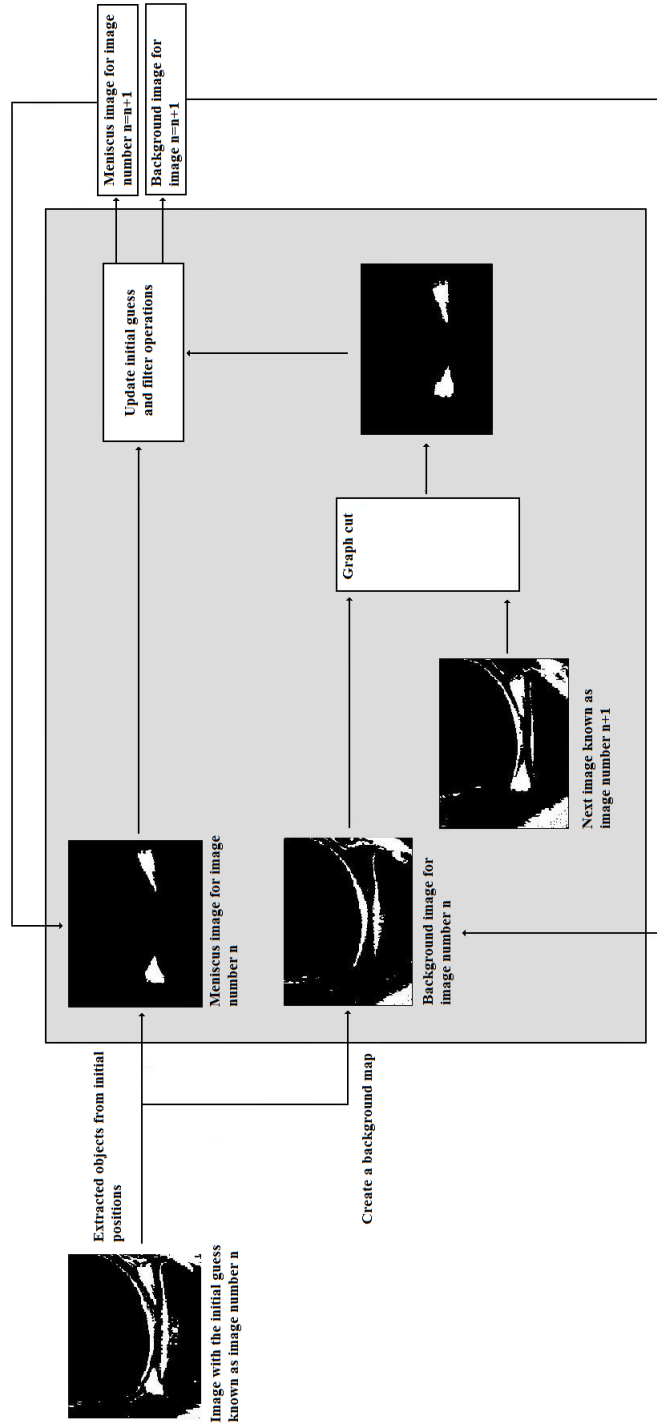


Figure 3.11: The figure shows the workflow for the segmentation of the menisci with the graph cut method.

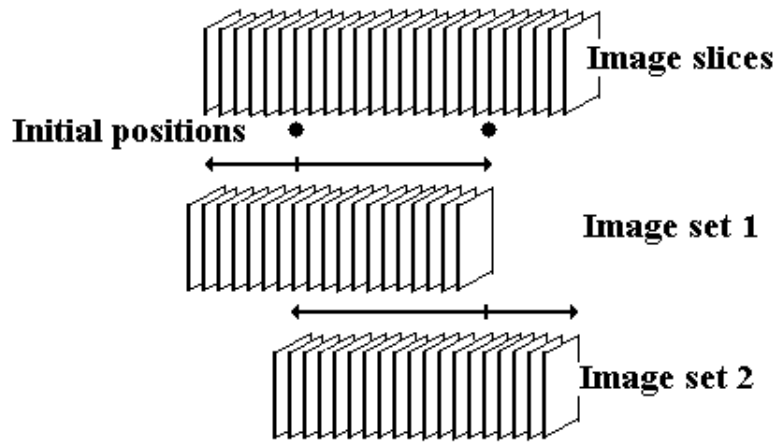


Figure 3.12: The small circles in the figure illustrate the two found initial position of the lateral and medial meniscus. From these position the search for the other parts of the menisci is done in the illustrated directions, i.e. totally four directions. From each initial guess a new image set will be created containing the result from the segmentation process from concerned images.

Chapter 4

Results

In this chapter the result from the different sub parts in the process of automatically segment the menisci is discussed. The workflow of this Masters' thesis was divided into three parts. The result from each part will be presented in one section each.

4.1 Result of Bone Segmentation

The purpose of segmenting the bone was to reduce noise in the images. This was done with texture classification. Laws' texture algorithm was used to extract features from different textures. Other methods such as first order statistics and Co-occurrence matrices with first order statistics were tried, cf. [2], with no success. In this section the result from the bone segmentation is discussed and therefore one essential part is how well the classification worked.

Some tissues and bone can be very similar and very hard to separate. This is visible in figure 4.1 where the left images illustrate the original MR image and the right image displays the result from the classification process, known as the probability map. The MR images approximately contain three textures. In the left image these textures are manually selected and classified as bone, bright tissue and dark tissue. As said earlier some texture is hard to separate and especially the textures bone and bright tissue. The result from how well the classifier works is presented in figure 4.2. The data is gathered from six examinations and contains approximately 4000 images from each of the three texture types. These texture images are extracted manually from the MR images to compare the result from the classifier with the result given by the user. The classifier calculates a probability that the texture present in the image is bone. This means that textures that are not bone will have a small probability. From this probability the system needs to decide a threshold value that can be used to classify the textures as either bone or not bone. Therefore, the accuracy of the classification for the three texture types is calculated against different threshold values. The result is shown in figure 4.2. The accuracy is how many of the

texture images that has been accurately classified in the system with the given threshold value.

There are essentially two things to mention in the figure. First, note how well the system works when differentiating the bone from the dark tissue in the threshold interval 0.45-0.65. In this case the dark tissue and the bone accuracy is above 90%. Secondly, note how difficult it is to separate the bright tissue from bone. In the interval 0-0.65 the bright tissue has an accuracy under 10% and bone has an accuracy above 90%. In the interval 0.70-1 bright tissue has an accuracy of above 90% and bone has an accuracy under 10%.

In the system the threshold was set to 0.5, see equation 3.2. One can argue that it might be better to have a slightly higher threshold to increase the accuracy of the dark- and bright-tissue as the bone accuracy is slightly stable. However, this is only slightly modifications and will not change the result remarkably.

Even if the classifier has problems to separate the bright tissue from the bone it does not impact the main objective to segment the menisci. These textures are hard to separate but they do not look similar to the menisci and therefore it does not matter if the bright tissue is classified as bone as long as it does not interfere with the menisci. So the objective is to segment the bone as well as possible without erasing any valuable information regarding the menisci, and this segmentation process works well with that objective.

Since the probability map is sufficiently accurate the graph cut method works very well. In figure 3.6 and 3.8 two examples of bone segmentation is presented. From these figures it is visible how well the bone segmentation works. In figure 3.6 it is also visible that brighter tissue is classified as bone, but as explained it does not matter since it is not similar to the meniscus textures and will not be in danger for bad classifications regarding the menisci. In the image in figure 3.8 the meniscus is zoomed in and the segmentation of bone around the meniscus is shown clearly.

4.2 Result from Locating the Menisci Locations

The objective of the second part was to reduce the image size to be able to localize the meniscus. This method is based on a superposition of the segmented bone images. The method for locating the meniscus area is based on a thresholding and histogram method of the superposition image. The result from this method depends on how well the bone classification went. Figure 4.3 shows the result from four examinations. As seen in this figure the area where the menisci can be located is found, often very well especially regarding the vertical position. The horizontal position is sometimes harder to find, see the lower image in the right column in figure 4.3. The purpose is still only to reduce the image size without losing information regarding the menisci to simplify the segmentation process.



Figure 4.1: The left figure illustrates regions of the three different texture types dark tissue, bright tissue and bone. To the right the image illustrates the created probability map where the intensity is based on how certain the system is that the region is bone. Note that the classifier can not separate the bright tissue from the bone.

4.3 Segmentation Result of the Menisci

The third part was the segmentation of the menisci and this process is much harder. The menisci and the cartilage in the neighborhood sometimes are joint together, see the lower image in the left column in figure 3.8. To lower these effects information from the nearest images is used to reduce this noise, see section 3.3.2. This process reduces the noise in the images and this is necessary due to the fact that the detected menisci objects is used to search for the meniscus in the nearby image. Noise will affect this search process and reduce the possibility to extract only real meniscus parts and create a 3D object of the menisci.

The segmentation result from five examination is shown in figure 4.4. In the images the lateral as well the medial menisci are presented. The medial meniscus is the upper meniscus in the images. In the segmentation process more filtering operations are needed to reduce the presence of cartilage when extracting the lateral menisci compared to the medial menisci. Therefore the medial menisci have a more homogeneous surface. Even if there are filter operations to reduce the cartilage sometimes they do not remove all. In the lower image in column one and the upper image in column two some cartilage is present. As discussed earlier the segmentation process uses information in the previous images to reduce noise. In some cases as the examination seen in column three, the image quality is not good enough. If the intensity is too similar around the menisci the system can not segment the menisci parts and no result is achieved. In this case the system can not distinguish the menisci from the rest of the image.

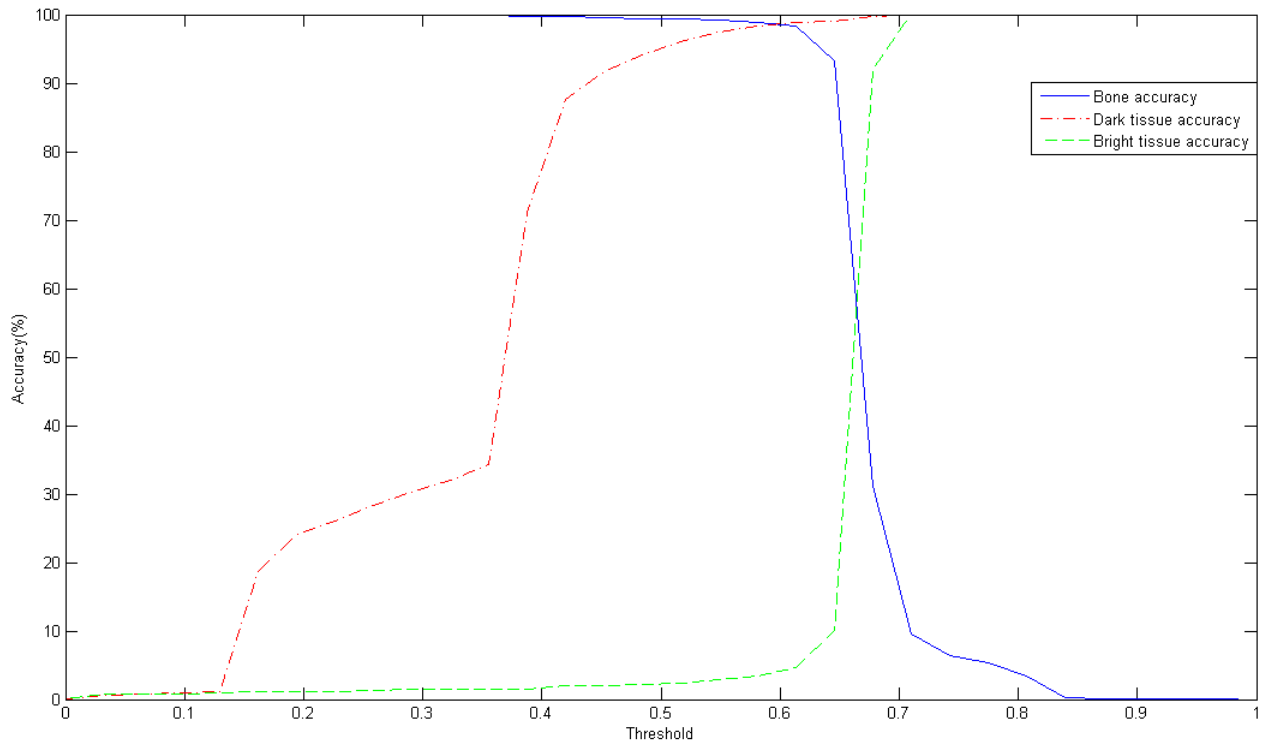


Figure 4.2: The figure illustrates how accurate the classification system works for three texture types when changing the threshold value for being classified as bone resp. not bone. The three texture types is dark- and bright-tissue and bone.

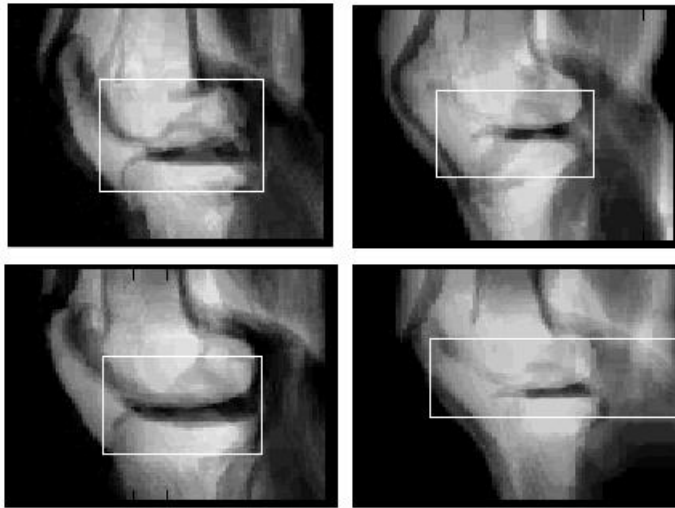


Figure 4.3: In this figure the superposition results from four examinations is displayed. The white squares illustrates the located menisci area calculated with a threshold and histogram based method. Note that especially the vertical position is found correctly and that the horizontal sometimes get a bit wider. However, the purpose of this calculation was to reduce the image size without losing any information about the menisci.

4.4 Evaluation of the Results from the Automatic Segmentation

In this thesis the automatic segmentation is tested on five examinations. To evaluate how good the result was Magnus Tägil at Department of Orthopedics in Lund, manually segmented the menisci in four of the five examinations and one examination twice. The area from the automatic segmentation process was then compared to the resulting area of the manual segmentation.

In the sagittal view the menisci will either be seen as one joint or two separate objects i.e. the posterior and anterior menisci parts, see figure 4.5. Therefore the evaluation compares the posterior and anterior parts slice by slice. In cases where the menisci are segmented as one object, the menisci object will be presented in both the evaluation for the posterior and anterior parts. This is shown in figure 4.6. The left column shows the menisci area from both the manual and automatic segmentation for the anterior menisci parts, slice by slice, i.e. both the lateral and medial menisci are present in these images. Vice versa the right column shows the posterior menisci area parts, slice by slice. The first four rows show the four examinations that are being compared. The last row compares the manual segmentation results from one examination at two different moments.

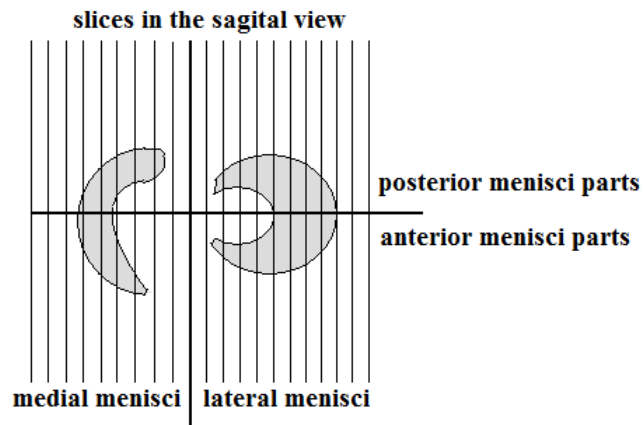


Figure 4.5: To evaluate how good the segmentation result became the result from the automatic segmentation process should be compared to the result from an manual segmentation. To do that the objects in the slices are divided into two parts, anterior and posterior menisci parts. This means that both the medial and lateral menisci are present in the anterior and posterior menisci parts.

4.4.1 Examination 1

The first row in figure 4.6 corresponds to the upper image in the left column in figure 4.4. In this case the initial guess for the medial meniscus is slice number 5 and slice number 22 for the lateral meniscus. As seen in the left column the automatic segmentation is slightly over segmented. In the right column the result shows that the automatic segmentation has segmented objects in slice number 10-14 that has not been manual segmented. In this case the menisci have an tubular structure that more or less links the medial and lateral menisci together. This is not really menisci parts, but the system can not differ these objects from the menisci. The result for the lateral meniscus is quite accurate in slice number 20-24. In figure 4.7 the segmentation result of slice number 5 is shown. The white objects is the result from the segmentation. The left image contains the result from the manual segmentation and the right the result from the automatic segmentation process. In this slice the segmentation result is very similar.

4.4.2 Examination 2

The second row in figure 4.6 belongs to the upper image in the second column in figure 4.4. Slice number 5 is the initial guess for the medial meniscus and slice number 18 is the initial guess to the lateral meniscus. As seen in these images the system have over segmented the menisci. This is due to noise or cartilage was present in these slices, especially in slice number 19-20 in the left column and slice number 6-9 in the right column.

4.4.3 Examination 4

Row number three in figure 4.6 corresponds to the examination in the lower image in the first column in figure 4.4. The initial guesses are slice number 4 and 21. The segmentation result shows that the automatic segmentation process also had issues with noise or cartilage in this examination. This is seen in slice number 5-8 in the right column. Also observe how close the segmentation results are to each other in slice 20-25. Figure 4.8 contains the segmentation result for slice number 7. The left image contains the manual segmentation result and the right the automatic. In this case the automatic segmentation has segmented a bigger area than the manual due to that automatic system can not distinguish the cartilage from the meniscus.

4.4.4 Examination 5

The fourth row in figure 4.6 belongs to the lower image in the second column in figure 4.4 were the initial guesses are slice number 10 and 19. The segmentation result is close to the manual segmentation result in slice number 4-9 in the left column and in 17-21 in the right column. The posterior meniscus parts from the medial meniscus is found in slice number 4-8 in the right column. In the same

slices the automatic segmentation could not find any menisci parts. The reason is that the system could not distinguish the meniscus part in the image. This is displayed in figure 4.9 which displays the segmentation result of slice number 5. In the left image the manual segmentation result is shown and in the right the automatic. In this case there are no posterior menisci parts segmented and this is due to the diffuse meniscus borders.

4.4.5 Examination 5 again

The last row in figure 4.6 shows the manual segmentation result from one examination produced at two different times. The interesting part is how different the result became. In this case the area variation differs a lot in some slices, almost 50% in slice number 20 in the right column. Also observe the difference in slice number 10 and 17 in the left column where menisci parts is found in one examination but not in the other. This shows how difficult the segmentation task really is and how much an accurate automatic segmentation process could help future diagnoses.

4.4.6 Summary

Overall the segmentation system is quite accurate in the neighborhood of the initial guesses. The system is not perfect and has some issues with cartilage and noise, in some slices, and deciding when to stop the search process. In several slices the segmentation has continued when the manual segmentation has stopped.

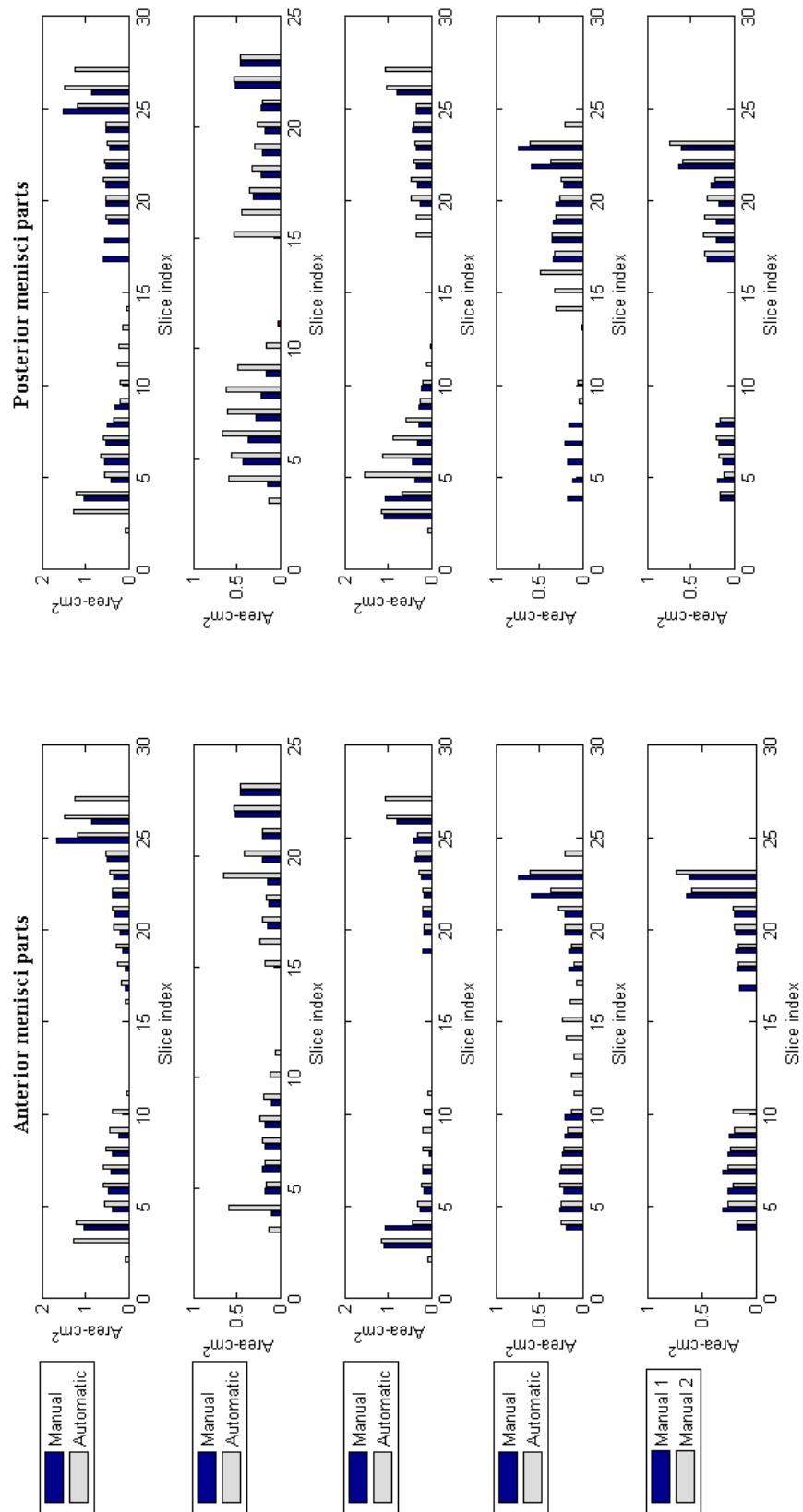


Figure 4.6: In this figure the area between the manual and automatic segmentation is displayed.

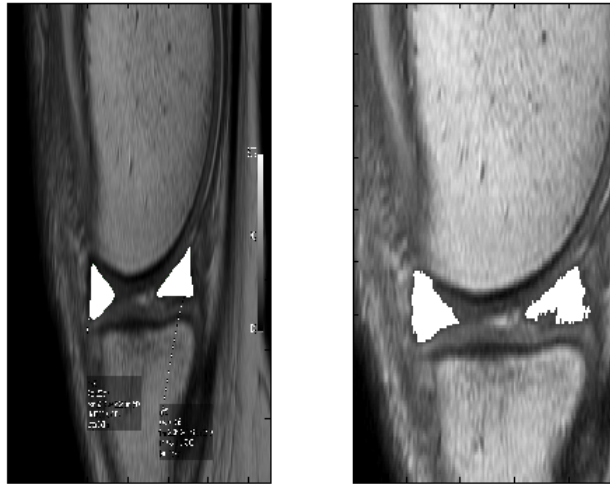


Figure 4.7: This image shows the segmentation result of the initial guess in examination 1, slice number 5. The left image shows the result from the manual segmentation and the right the automatic. The segmentation result is plotted as white objects. Please note that the images have different scales because the manual segmentation was done in an external program.

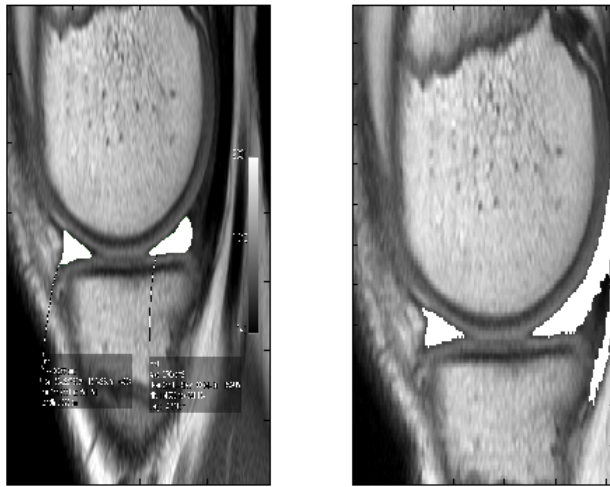


Figure 4.8: The left image shows the manual segmentation of slice number 7 in examination 4. In the right image the segmented area from the automatic segmentation is shown. The segmentation result is plotted as white objects. Please note that the images have different scales because the manual segmentation was done in an external program. In this case the segmentation result have had trouble with distinguish the meniscus borders, which resulted that bigger area was segmented.

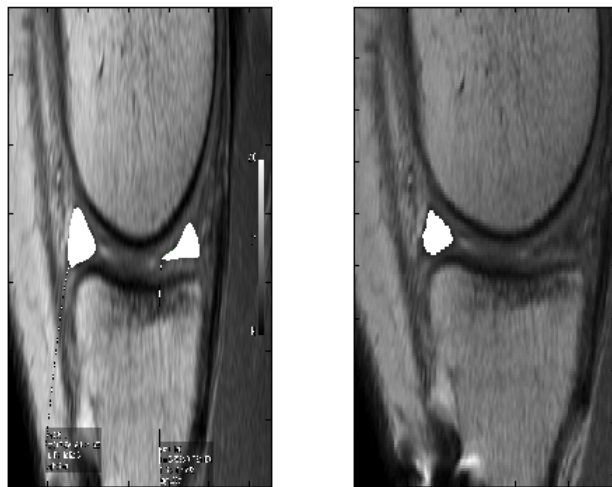


Figure 4.9: The manual segmentation result for slice number 5 in examination 5 is shown in the left image. The result is displayed as white objects in both the left and right image. In this case the automatic segmentation could not segment the posterior meniscus part, see the right image. This is due to the diffuse borders of the meniscus. Note that the images have different scales.

Chapter 5

Future work

The approach to automatically segment the menisci in this Masters' thesis uses some different search methods and these can be very time consuming in Matlab. This program was not constructed to be very fast, but as an improvement the search methods could be written in a faster programming language.

At the moment the program is constructed to work with MR images with the image acquisition discussed in section 1.3. This means that the training data used when segmenting bone is limited to this image acquisition. More training data could make this program work with additional examinations with other image acquisitions.

As discussed in the result chapter the whole workflow demands that the bone segmentation works well. To improve this segmentation the classifier could be tested for optimization. Perhaps not all 71 features are necessary to use and perhaps a better result would be achieved by replacing the k-nearest neighbor with another classifier such as support vector machine [1, page 523-527].

At the moment the segmentation process used is a bit complex. One problem with the segmentation process used in this thesis is that cartilage interfere with the segmentation process and influences the result. Perhaps a better result could be achieved with a 3D graph cut segmentation. Usually the cartilage around the tibia are joined together with the menisci, as seen in lower image in the left column in figure 3.8. This will of course influence the result in the segmentation process. A 3D graph cut segmentation might reduce this phenomena since the cartilage shape is thin and wide and might be limited in the regularization term. This could result in a more accurate segmentation. Even better result would probably be achieved if the segmentation system used graph cut with shape priors. The menisci has a known shape and that could be used to create shape priors. Another approach would be to modify the existing program by updating the mean intensity in every slice before the graph cut segmentation. This could perhaps result in a more accurate segmentation. The segmentation process in this thesis uses a calculated converged mean intensity of the meniscus in the segmentation process for all slices.

The main objective is to use the 3D object to determine if the menisci are

healthy or not. This would involve a pattern recognition system to classify the menisci as healthy or not. Some studies have already been done that can be used as an inspiration to suitable features that can be used in such classifications, cf. [21]. Features of interest would most certain be features like the volume, surface and determine if the menisci horns are sharp or truncated. The features would probably depend on factors like gender, age and body mass.

Bibliography

- [1] David A. Forsyth and Jean Ponce. *Computer Vision: A Modern Approach*. Alan Apt, 2003.
- [2] E. Alegre, V. Gonzalez-Castro, S. Suarez, and M. Castejon. Comparison of supervised and unsupervised methods to classify boar acrosomes using texture descriptors. *2009 International Symposium ELMAR*, pages 65–70, 2009.
- [3] I. Boniatis, G. Panayiotakis, and E. Panagiotopoulos. A computer-based system for the discrimination between normal and degenerated menisci from Magnetic Resonance images. *2008 IEEE International Workshop on Imaging Systems and Techniques*, pages 335–339, 2008.
- [4] Y. Boykov and R. Veksler, O. Zabih. Fast approximate energy minimization via graph cuts. *IEEE Transactions on PAMI*, 23(11):1222–1239, 2006.
- [5] Yuri Boykov and Vladimir Kolmogorov. Implementation of maxflow-v3.01, 2010. <http://www.cs.ucl.ac.uk/staff/V.Kolmogorov/software.html>.
- [6] M.D Crema, A Guermazi, L. Li, M.H Nogueira-Barbosa, and et al. The association of prevalent medial meniscal pathology with cartilage loss in the medial tibiofemoral compartment over a 2-year period. *Osteoarthritis and Cartilage*, 18(3):336–343, 2010.
- [7] Omer Demirkaya, Musa Hakan Asyali, and Prasanna K.Sahoo. *Image Processing with MATLAB, Applications in Medicine and Biology*. Boca Raton : CRC Press, 2009.
- [8] J. Fripp, P. Bourgeat, C. Engstrom, S. Ourselin, S. Crozier, and O. Salvado. Automated segmentation of the menisci from MR images. *2009 IEEE International Symposium on Biomedical Imaging: From Nano to Macro*, pages 510–513, 2009.
- [9] J Fripp, S Crozier, S.K Warfield, and S. Ourselin. Automatic segmentation of articular cartilage in magnetic resonance images of the knee. *IEEE Transactions on Medical Imaging*, 29:55–64, 2010.

- [10] Jurgen Fripp, Stuart Crozier, Simon Warfield, and Sebastien Ourselin. Automatic segmentation of the bone and extraction of the bone-cartilage interface from magnetic resonance images of the knee. *Physics in Medicine and Biology*, 52(6):1617–1631, 2007.
- [11] Y. Hata, S. Kobashi, Y Tokimoto, M. Ishikawa, and H. Ishikawa. Computer Aided Diagnosis System of Meniscal Tears with T1 and T2 Weighted MR Images Based on Fuzzy Inference. *Computational Intelligence. Theory and Applications*, LNCS 2206:55–58, 2001.
- [12] Klas Josephson. Segmentation of Magnetic Resonance Images of the Knee using Tree-dimensional Active Shape Models. Master’s thesis, Dept. of Mathematics, Lund Institute of Technology, Sweden, 2004.
- [13] V. Kolmogorov and R. Zabih. What energy functions can be minimized via graph cuts? *IEEE Transactions on PAMI*, 26(2):147–159, 2004.
- [14] C. Kose, O. Gencalioglu, and U. Sevik. An automatic diagnosis method for the knee meniscus tears in MR images. *Expert Systems with Applications*, 36(2):1208–1216, 2009.
- [15] Ian D. McDermott. What tissue bankers should know about the use of allograft meniscus in orthopaedics. *Cell and Tissue Banking*, 11(1):75–85, 2010.
- [16] B. Paniagua-Paniagua, M.A. Vega-Rodriguez, and P. Bustos-Garcia. Advanced Texture Analysis in Cork Quality Detection. *2007 5th IEEE International Conference on Industrial Informatics*, pages 311–315, 2007.
- [17] R. Pfisterer and F. Aghdasi. Comparison of texture based algorithms for the detection of masses in digitised mammograms. *AFRICON, 1999 IEEE*, 1:383–388, 1999.
- [18] M. Rachidi, C. Chappard, A. Marchadier, C. Gadois, and et al. Application of Laws’ masks to bone texture analysis: An innovative image analysis tool in osteoporosis. *2008 5th IEEE International Symposium on Biomedical Imaging: From Nano to Macro*, pages 1191–1104, 2008.
- [19] M.T Suzuki, Y. Yaginuma, and H. Kodama. A texture energy measurement technique for 3d volumetric data. *2009 IEEE International Conference on Systems, Man and Cybernetics*, pages 3779–3785, 2009.
- [20] M.S. Swanson, J.W. Prescott, T.M. Best, K. Powell, R.D. Jackson, F. Haq, and M.N. Gurcan. Semi-automated segmentation to assess the lateral meniscus in normal and osteoarthritic knees. *Osteoarthritis and Cartilage*, 18(3):344–353, 2010.
- [21] W. Wirth, R.B. Frobell, R.B. Souza, X. Li, B.T. Wyman, M.P Le Graverand, T.M. Link, S. Majumdar, and F. Eckstein. A three-dimensional quantitative method to measure meniscus shape, position, and signal intensity using

mr images: a pilot study and preliminary results in knee osteoarthritis.
Magnetic resonance in medicine, 63(5):1162–1171, 2010.

- [22] Donald W. McRobbie, Elizabeth A. Moore, Martin J. Graves, and Martin R. Prince. *MRI from picture to proton*. printed in the United Kingdom at the university Press, Cambridge., second edition, 2008.